

CONTENT:

Table 1 (coordinates),	p. 2
Table 2 : description of the sedimentary record (Rangá valley),	p. 3
Table 3: Dating	p. 7
Analytical technics.	P. 11
Illustrations (Rangá valley, Bitra earthquake and Kleifarvatn),	p. 12

Table 1 Location of the investigated sites in the Rangá valley

Place	Base of the outcrop (m)	Top of the outcrop (m)	Latitude (N)	Longitude (W)
Akbraut	71	82	64°00'23.60"	20°22'12.78"
Buði morainic arc (þjórsá)	95	-	64°00'56.80"	20°16'31.23"
Bolstaður (R-C6)	40	42	63°54'52.02"	20°51'47.19"
(þjórsá) Units R-C2-C3	125	130	64°04'59.16"	19°53'34.25"
Galtalækur (II) unit R-B2a	106	130	63°59'26.29"	19°52'09.08"
Galtalækur (II) Unit R-C4 (lava)	113	117	64°00'00.5"	19°56'09.88"
Heiðarbrekka West	71	80	65°54'46.64"	20°13'16.78"
Heiðarbrekka East Vikingalækur river	75	75	65°54'45.44"	20°12'16.78"
Kirkjubær	35	39	65°50'29.00"	20°21'22,75"
Lambagi (þjorsa) Units R-C1-C2-C3	125	130	64°05'22.00'	19°56'24.57"
Litlilækur Old basalt dating/below R-C2		110	63°58'32.67"	19°57'36.32"
Næfurholt unit R-B2 Unit R-C2	120 variable	124 variable	63°59'13.89 63°59'18.0	19°55'55.93" 19°57'70.0"
Ofærugill units R-C1-C2-C3	202	207	64°03'48.12"	19°45'32.29"
Skarösfjall			64°01'56.20"	20°06'45.48"
Syðristapi	143	165	63°59'35.70	21°59'52.97"
Vikingalækur Unit R-C3a	88	92	63°54'51.79"	20°09'38,05"

Table 2 : Lithostratigraphic description of the Ytrí Rangá sedimentary sequence, co-seismic deformations, tectonic and dating

Mem..	Unit /subunit	Facies	Interpretation	Co-seismic activity / faulting	Volcanic activity	Climatic context / Age
F		Coarse grey sand , poorly stratified , discrete or fluvio-glacial deposits within incision	Aeolian dunes sandur with recurrent jökulhlaups	faulting, rock falls, water escape features and collapsed thufurs on the Vorðufel	Many tephra , including	Little Ice Age Subboreal
		2 to 5 m of unconsolidated stratified silty loam	Loesses (Jackson et al., 2005)		Many tephra , including H1, H3, H4,H5	Younger than 8.500 cal BP (Jackson et al., 2005)
		Large sand splays were fed by glacial rivers with poorly sorted gravels and incision	<i>sandur</i>		Veidivötn lava flow : Þjórsá lava's, not faulted	ca 8.600 cal BP
E	E2	Large sand splays were fed by glacial rivers with poorly sorted gravels and incision	Sandur with Recurrent jökulhlaups	Saksunarvatn tephra (10,3-9,9 ka) Faulted lava along Skarösfjall FS. (Fig. 7A and B) in the Ytri Rangá valley Massive graded gravels in a raised beach at Þjóðolfshagi (Fig. 7D).	Lava flow lapping on the Búði moraine	REGRESSION (ca 11cal ka)
		Clayey tillites (terminal moraine)	Sandur with Recurrent jökulhlaups			Preboreal Budi Advance (11,2 cal ka)
		Sandy sedimentation outside the former morainic arcs and even cobbly on isles. Rhythmic silty to clayish including shells marine silty clay deposits re-working the Vedde Ash. ----- Tillites including the Vedde Ash at its top	Marine sedimentation Terminal moraine Recurrent jökulhlaups (11,5 ka)	Recurrent small sized (5-10 cm diam.) loadcast or oriented sub aquatic Kelvin Heimholz convolutess; fragmented folded beds.		MFS Termination Ib Younger Dryas: Mykjunes /Pula advance (13-11,7 ka)
		Large sand splays were fed by glacial rivers with poorly sorted gravels and incision; ----- Rhythmic silty lacustrine sedimentation		Recurrent small sized loadcast or oriented sub aquatic Kelvin Heimholz convolutess	Lava flow	Bölling –Alleröd deglaciation (Termination Ia)

	E1	Rarely preserved relicts of matrix supported tillites	basal tills			Late Weichselian
D	D2	Rarely preserved relicts of basal tills remolding grey fluvio-glacial sand with rare cobbles and blocks, further deformed by both glaciectonics, lying on an erosional discontinuity.	Glacial advance	<i>fault rupture on SISZ</i> (at Heiðarbrekka-East (N150° and N20)		Early Weichselian GS 21
	D1	Fluvio-glacial conglomerate	Sandur			Glacial advance upstream (GS 22)
C	C6 Mostly restricted to the Ytri- and Estry-Rangá lower watersheds..	very late stratified silty loams with trace of runoff, at Hellar Cave. pseudogley soil and loesses	Colluvium on loess sandur		thick reworked basaltic tephra from Grimsvötn and Hekla/Katla signature (microprobe) equating the 110 ka NGRIP 2745.60 m	110 ka (GI 23) Glacial advance upstream (GS 23)
		highly variable: set of stratified coarse sands in throughs and large channels with oblique cross stratifications, with herringbone fabric and rare tidal vails and no bioturbation at Bólstaður . Reworks gravels and clasts from the already consolidated older units.	top set of a Gilbert delta at Bólstaður.			EMERSION REGRESSION GS 24
		Tidal rhythmites at Heidarbrekka. It is present as tidal rhythmites resting on -C5 (loess) at 165 m a.s.l. in the Skarðsfjall. major incision	Jökulhlaups Second marine highstand, forced by glacio-isostasy Jökulhlaups	Syn-sedimentary faulting at Heidarbrekka.(Hekla F.S.)		MFS2 (115 ka): GI 25 TRANSGRESSION 2
	C5 Restricted to the Ytri Rangá and Þjórsá valleys	laminated yellowish silty sand deposits, relatively wavy, with rhythmic silts and silt sands with rusty rooting in the upper 30cm, followed by 20 cm of cross stratified sands in low positions. Base clear and wavy	Wet aeolian loesses with some flooding evidence	No evidence of convolutes nor fracturation	Several centimetre to decimetre basaltic tephra layers interstratified with 10 thinner one .	EMERSION GS26/ C25
	C4 Restricted to the Ytri Rangá and Þjórsá valleys and the Skarðsfjall	The top is commonly weathered by an hydromorphic palaeosol. Finely stratified rhythmic silts and silt sands with rooting and burrows and iron hydroxide staining. Evidence of synsedimentary frost activity The base is very irregular and clear,	Tidal flat evolving into a tidal marsh	The top part is associated with a fault rupture with large intraclasts of tidal rhythmites Often deformed by oriented or irregular convolutes of various size followed to depth by dish-like structures penetrating into subunit R-C3a. Locally folding can be observed.	At Galtalækur, (120 m a.s.l.), a thin (<2 m) but extensive basaltic lava flow from the Hekla volc. spreaded over an internal erosion surface during the early period of sedimentation; with a tumuli surface morphology and large polygons	ONSET OF REGRESSION GS26/ C26

				Major earthquake on the SISZ F.S.	(inflated lava flows).	
	C3 Restricted to the Ytri Rangá and Þjórsá valleys and the Skardsfjall	Set of sands in throughs and flats with tidal vails herringbone fabric and rare bioturb-ations. R-C3a is rather fine and rythmic, in flats. R-C3b consists in large channels with oblique trough-cross stratifications. The base is irregular and clear	Tidal flat with tide channels in a widespread deposition during a still active transgressive pulse (above 60 a.s.l. to 215 m on the Skardsfjall) <i>jökulhlaup</i> activity.	At Kirkjubær (Fig. 6), deformed by plurimetric convolutess, certainly of co-seismic origin .At Heiðarbrekka, deformed by load casts, dish structures, injected flame structures and verti-cal pipes features from the upper boundary (Fig. 4). The water escapes and clastic dykes at advocating major seismic events at the end of the sedim-entation.. Brittle fracturing , deforms most of the unit in a transtensive regime, related both with the Hekla and the SISZ fault systems (Figs. 3 and 4).	reworks a large amount of phreatomagmatic tephra from the Grímsvötn volc. (C3a) (microprobe), splayed above 70 m a.s.l. at c. 127 ka Correlated with 5e Bas Low tephra	THERMAL OPTIMUM, 127 ka MFS 1 (ca 126 ka)
	C2 Restricted to the Ytri Rangá and Þjórsá valleys	2 to 5 m of cross stratified sands bodies, locally associated with mud vails Syn-sedimentary convolutess; regularly pierced by vertical sandy pipes and lately (post consolidation) de-formed by transtensive faulting in horizontal section (Fig. 3).	sandy fluvial channel deposits within a braided fluvial network with some tidal influence downstream (<140 m a.s.l.) under a microtidal regime. Coastal fluvial deposits suggesting a progradation of marine deltaic bodies corresponding to an early regression with erosion of the substratum inland in connection to the glacial rebound. <i>jökulhlaup</i> scouring	Water-escape pipes are very frequent, at the crossing of both directions (Fig. 4 and 5). Convolutess and water-escape structures are also pre-sent in some places as in front of the Búrfellstöð power plant or at Lambagi along the Þjórsá River. Brittle fracturing , deforms most of the unit in a transtensive regime, related both with the Hekla (dominant) and the SISZ fault systems (Figs. 3 and 4). Hekla system is N40° to N60°, SISZ fault trends range between N10°and N155° following the sites.	Top of the formation: distal rhyolitic tephra of the Hekla volcano plinian eruption , 60 cm thick, pasting on an heated (rubified) palaeo-surface (jökulhlaup scouring), followed by water reworked pumice and basaltic tephra, evolving glacialfluvial (base of C3b; p.12)	Early MIS 5e TRANSGRESSION 1
	C1 Restricted to the Ytri Rangá and Þjorsa valleys	b) rhythmite coarsely stratified gruss and gravels reworked from R-B2 a) conglomerate and sands, crosstratified, rework an old Hekla pumice	hyperpycnal flows deposits emplaced in a proglacial lake , pulsed by recurrent jökulhlaups ; emplaced below140 m a.s.l.; Sandur with jökulhlaups above 140 ml	Syn-sedimentary water-escape structures. Brittle fracturing (Hekla Fault.System only)	Not found	Final deglaciation
B	B3 Restricted to the upper Ytri Rangá valley	silty rhythmites preserved at Næfurholt, . Erosion surface	Juxtaplacial Jökulhlaup	Oriented (NE) syn-sedimentary Kelvin-Helmholtz convolutess.	Not found (limited outcrop)	Deglaciation MIS 6
	B2	B2c : coarsely stratified till with dropped blocks, covered unconformably by stratified rhythmites	Deformed by late glaci-tectonism brief glacial re-advance damming a subglacial			MIS6a (GM)

	Restricted to the upper Ytri Rangá valley	deformed by glaciectonic. Erosion surface	lake and further emerged in the form of an aerial lacustrine episode Jökulhlaup			
		B2b: stratified prograding fan and further by a slurry flow reworking a phreatomagmatic advance cone of the Hekla volcanic system. Erosion surface	Mass wasting Jökulhlaup		The phreatomagmatic cone likely emerging from the glacier at and was further destabilized during glacier melting (van Vliet-Lanoë et al., 2018).	MIS6b interstadial
		B2a: begins with subglacial pillow lava flows partly brecciated to the top jökulhlaup activity.			Norðbjallar hyaloclastite ridge, 500 m a.s.l., Hekla Veidivötn (⁴⁰ K- ⁴⁰ Ar 155 ka)	MIS 6c
	B1 Restricted to the upper Ytri Rangá valley	Tills, locally faulted and lately incised to the present valley floor by				MIS 6c?
A	A Restricted to the upper Ytri Rangá valley	It consists in highly consolidated dark-grey tills and basaltic lava flows (the Oldest Basalts, OB) and are incised, glacially polished, faulted.	These deposits are unconformably covered by matrix-supported basal tills (R-B1-2) and/or by other younger deposits of the Eemian Member (R-C).			age is older than MIS 6.

OTHER HYALOCLASTITE RIDGES

To the east of the SISZ, in addition to the hyaloclastite ridge of Hellutindar and in parallel with the Laki and Eldja ridges, other hyaloclastite ridges seem from our field observations to have also formed during the MIS 6b minor deglaciation, in agreement with the source and dating of the lava flows in the Ytri Rangá Valley (Litlælækur; Table 2). In the eastern part of the Veidivötn fault system at Lake Austurbjallavatn (right bank of the Tungnaá River; Fig. 1B) the consolidated, weathered and faulted character of the sediments (MIS 5e alluvial fan) overlapping the Snjóöldufjallgarður ridge (hyaloclastites and pillow lavas; Fig. 1B) also suggest major fissural activity just prior to the MIS 5e deposits. A similar situation seems to apply to the Þoristindur ridge, at the western end of the Veidivötn fault system, to the stacked pillow lava flows prior to the last tillites (Last Glacial) visible at Sigöldufoss, and at the outlet of Þorísvatn (Fig. 1B). Other ridges, overlapped by MIS 5e faulted alluvial fans seem to have been synchronously active to the east, in the upper Markarfljót area, south of the Torfajökull fault system, a prolongation of the Grímsvötn fault system (Fig 1A; unsuccessfully dated). These include the Hagafell and Tveggjar hyaloclastite ridges, which appear to be relatively fresh, and buried with large sedimentary deformed by glaciectonism, similar in facies to those of the Last Interglacial formation (consolidated, faulted).

DATING

Uranium – Thorium

Whole rock and mineral separates were spiked with a ^{229}Th - ^{233}U - ^{236}U mixed double-spike, then dissolved with HF HNO₃ and HCl. U and Th analyses have been done after chemical isolation of U and Th at BRGM Orléans on a "Neptune" MC-ICPMS mass spectrometer. Details on chemical separation and mass spectrometry can be found elsewhere (Innocent et al., 2005; Millot et al., 2011)

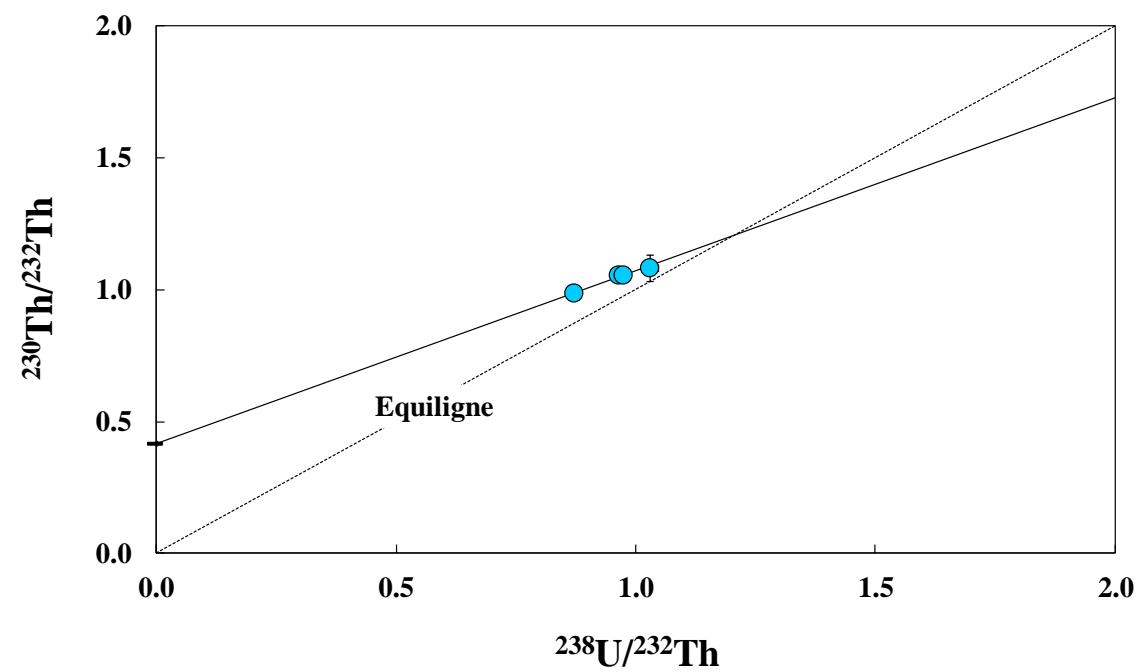
Total blanks were 42 pg for U and 232 pg for Th.

Results are reported in the following table. Uncertainties (in parentheses) are given as 2σ

Sample		U ($\mu\text{g/g}$)	Th (ng/g)	($^{234}\text{U}/^{238}\text{U}$)	($^{238}\text{U}/^{232}\text{Th}$)	($^{230}\text{Th}/^{232}\text{Th}$)	($^{230}\text{Th}/^{238}\text{U}$)	($^{230}\text{Th}/^{234}\text{U}$)
Ranga 1	whole rock	0.5226 (17)	1644 (10)	0.9999 (39)	0.9646 (69)	1.0534 (124)	1.0927 (78)	1.0928 (78)
Ranga 2	whole rock	0.3792 (17)	1180 (07)	1.0008 (83)	0.9753 (72)	1.0535 (135)	1.0812 (80)	1.0803 (80)
Sydra 3	whole rock	0.4380 (10)	1524 (03)	0.9973 (57)	0.8719 (27)	0.9853 (91)	1.1311 (35)	1.1342 (35)
ISLN 186 - 1	olivine	0.0257 (09)	98 (01)	0.9985 (250)	0.7927 (136)			
ISLN 186 - 2	matrix	0.0450 (03)	254 (02)	1.0068 (179)	0.5387 (64)			
ISLN 186 - 3	feldspar	0.0183 (02)	31 (01)	0.9919 (212)	1.7815 (187)			
ISLN 186 - 4	whole rock	0.4068 (23)	1198 (18)	1.0039 (43)	1.0305 (162)	1.0814 (498)	1.0508 (165)	1.0467 (164)

It has not been possible to measure Th isotopes in mineral separates, due to the very low Th concentrations and the amount of available material. All uranium activity ratios are at secular equilibrium. Whole-rock data have been reported on a ($^{238}\text{U}/^{232}\text{Th}$) – ($^{230}\text{Th}/^{232}\text{Th}$) isochron diagram (figure below).

The four datapoints plot on a straight line, but they are too clustered for a true isochron to be derived statistically. Nevertheless, calculations have been done using the method of Minster et al. (1979). A reference age of 116 ± 3 ky has been derived, with a MSWD of 0.23. The Y-intercept gives an initial ($^{230}\text{Th}/^{232}\text{Th}$) ratio of 0.42.



The obtained “age” is likely reliable. However, based on this dataset, it is believed that, the uncertainty may be underestimated.

Table 3 . Available dates of subglacial volcanoes used for figure 10

Site (see Fig. 1B and C)	Sample ID	Age $\pm 2\sigma$ ka	Method	Zone	
Hlöðufell tuya	ISLN-73 subglacial	118 \pm 17	K-Ar	Langjökull	Van Vliet-Lanoë et al., 2018
Hvalfell	Middle of the tuya	41 \pm 25	³⁹ Ar/ ⁴⁰ Ar	Langjökull	R. Duncan (unpublished, personal communication to A.Gudmundsson)
Jökuldalsheiði	ISLN-54, subaerial	155 \pm 36	K-Ar	Bruarjökull–Háslón	Guillou et al., 2010
Kerlingarfjöll	Fannberg	40.1 \pm 20	⁴⁰ Ar/ ³⁹ Ar	Hofsjökull	Flude et al., 2008
Kerlingarfjöll	Hvera	77 \pm 19.2	⁴⁰ Ar/ ³⁹ Ar	Hofsjökull	Flude et al., 2008
Kerlingarfjöll,	Hvera	117 \pm 22	⁴⁰ Ar/ ³⁹ Ar	Hofsjökull	Flude et al., 2008
Kerlingarfjöll	Mænir	125 \pm 24 124 \pm 38	⁴⁰ Ar/ ³⁹ Ar	Hofsjökull	Flude et al., 2008
Kerlingarfjöll	Hvera	151.1 \pm 11.6	⁴⁰ Ar/ ³⁹ Ar	Hofsjökull	Flude et al., 2008
Kerlingarfjöll	Snækollur ISLN-95; subaerial lava	149 \pm 3	⁴⁰ Ar/ ³⁹ Ar	Hofsjökull	Guillou et al., 2019
Kleifarvatn (Reykjanes)	Hellutindar; ISLN-109 Subglacial, HR	155 \pm 58	K-Ar	(Reykjanes)	Van Vliet-Lanoë et al., 2018
Kraþla	Hrafrthinnuhryggur	“24”	K-Ar	NVZ	Sæmundsson et al., 2000
Kraþla (liparite)	Taðfelli & Jörundur	80 \pm 3 85 \pm 1 90 \pm 3	K-Ar	NVZ	Sæmundsson et al., 2000
Kraþla (liparite)	Hagong (Halarauður)	112.5 \pm 3	K-Ar	NVZ	Sæmundsson et al., 2000
Ljósufjöll summit	02/102, L13 Unit 5 subglacial,	129 \pm 16	⁴⁰ Ar/ ³⁹ Ar	Snæfellsness	Flude et al., 2008
Ljósufjöll (Nykuhraun)	ISLN-99 subaerial lava	129 \pm 4	K-Ar	Snæfellsness	Van Vliet-Lanoë et al., 2018
Ljósufjöll summit	02/080 Unit 4, subglacial	113 \pm 6	⁴⁰ Ar/ ³⁹ Ar	Snæfellsness	Flude et al., 2008
Ljósufjöll (Gerðuberg)	ISLN-46, subaerial lava	135 \pm 5	K-Ar	Snæfellsness	Guillou et al., 2010
Pétursey tuya (10 km south of	ISLN-81 subglacial	113 \pm 5	K-Ar	Katla (Mýrdaljökull)	Van Vliet-Lanoë et al., 2018

Prestahnúkur tuya	Subglacial,	132 ± 19	⁴⁰ Ar/ ³⁹ Ar	Langjökull	Clay et al., 2015
Pórsmörk	Subaerial lava	55.6 ± 2	⁴⁰ Ar/ ³⁹ Ar	Torfajökull	Guillou et al., 2019 ; Moles et al., 2019
Rauðafell tuya West of the Hvítá River	ISLN-71 subglacial	104 ± 31	K-Ar	Langjökull	Van Vliet-Lanoë et al., 2018
Sandfell–Háslón	Dyke	150 ± 9	⁴⁰ Ar/ ³⁹ Ar	Bruarjökull - Háslón	Helgason and Duncan, 2003
Sandfell summit–Háslón recent dyke	KH1 subglacial	103 ± 17	⁴⁰ Ar/ ³⁹ Ar	Bruarjökull -Háslón	Helgason and Duncan, 2003
Skardsengi (Morðudalur, NVZ) above Syðra Fm.	ISLN-17 subaerial lava, H.R	81 ± 9	K-Ar	Morðudalur	Guillou et al., 2010
Skálamælifell	Post-Blake event	94.1 ± 7.8	⁴⁰ Ar/ ³⁹ Ar	Reykjanes	Jicha et al., 2011
Torfajökull	Bláhnúkur subglacial	108 ± 22	⁴⁰ Ar/ ³⁹ Ar	Vatnajökull	Clay et al., 2015
Upptypingar tuya	ISLN-59 subglacial	48 ± 7	K-Ar	Heirðubreið	Guillou et al., 2010
Upper Ytri-Rangá valley Lítlalækur	ISLN-84 subaerial	155 ± 25	K-Ar	Hekla	Van Vliet-Lanoë et al., 2018

References

- Clay, PL, Busemann, H, Sherlock, SC, Barry, TL, Kelley, SP, McGarvie DW (2015). ⁴⁰Ar/³⁹Ar ages and residual volatile contents in degassed subaerial and subglacial glassy volcanic rocks from Iceland. *Chemical Geology* 403:99–110
- Flude, S., Burgess, R., McGarvie, D.W. 2008. Silicic volcanism at Ljósufjöll. Iceland: insights into evolution and eruptive history from Ar-Ar dating. *Journal of Volcanology and Geothermal Research* 169:154–175.
- Guillou, H., Van Vliet-Lanoë, B., Guðmundsson, Á., Nomade, S. 2010. New unspiked K–Ar ages of Quaternary sub-glacial and sub-aerial volcanic activity in Iceland. *Quaternary Geochronology* 5(1):10–19.
- Guillou, H., Scao, V., Nomade, S., Van Vliet-Lanoë, B., Liorzou, C. and Guðmundsson, Á., 2019, ⁴⁰Ar/³⁹Ar dating of the Thorsmork ignimbrite and Icelandic sub-glacial rhyolites. *Quaternary Science Reviews*, 209, 52–62, doi.org/10.1016/j.quascirev.2019.02.014
- Jicha, B.R., Kristjánsson, L., Brown, M.C., Singer, B.S., Beard, B.L., Johnson, C.M. 2011. New age for the Skálamælifell excursion and identification of a global geomagnetic event in the late Brunhes chron. *Earth and Planetary Sciences Letter*, 310 (3-4), 509-517.
- Helgason, J., Duncan, R.A., 2003. Ar-Ar age dating of the Kárahnjúkurr volcanic formation, Kárahnjúkar. Hydroelectric Project, Age dating performed by dr. Robert A. Duncan. Jarðfræðistofan, Ekkra Geological Consulting Report LV–2003/090, 39 pp.
- Sæmundsson, K., Pringle, M., Harðarson, B.S. 2000. Umaldur berglaga I Kröflukerfinu. *Jærfræðafélag*, 13: 26-27.

DEM REALISATION FROM DRONES IMAGES.

The MicMac processing chain was used to compute the DEMs and orthoimages (OImS) from the drone images. The products were then georeferenced, using ground control points acquired by differential GPS in the field. In general, the absolute planimetric precision was better than 5 cm (or two pixels) and the altimetric precision was better than 5 pixels. The relative precision (error between one pixel and its neighbours) was better than 1 pixel in both plan and elevation.

MICROPROBE

Major element composition of phenocrysts in selected samples was determined by a CAMECA CAMEBAX SX100 electron microprobe at the Laboratoire Géosciences Océan (University of Brest) using a 15 kV and 10 nA beam focused to a spot of ~2 μm in diameter. The peaks were counted for 10s and backgrounds for 5 s. Light elements were counted first to preclude loss by volatilization. Oxides, natural mineral and synthetic standards have been used. Matrix corrections were performed by the PAP-procedure in the CAMECA software. Analytical precision (± 2 sigma error) evaluated by repeated analyses of individual grains is better than $\pm 1\%$ for elements with concentrations ≥ 20 wt% oxide, better than $\pm 2\%$ for elements in the range 10–20 wt% oxide, better than 5% for elements in the range 2–10 wt, % oxide, and better than 10% for elements in the range 0.5–2 wt, % oxide.

ILLUSTRATIONS

SEDIMENTARY FORMATIONS AND DEFORMATIONS, RANGÁ VALLEY



A



B



C



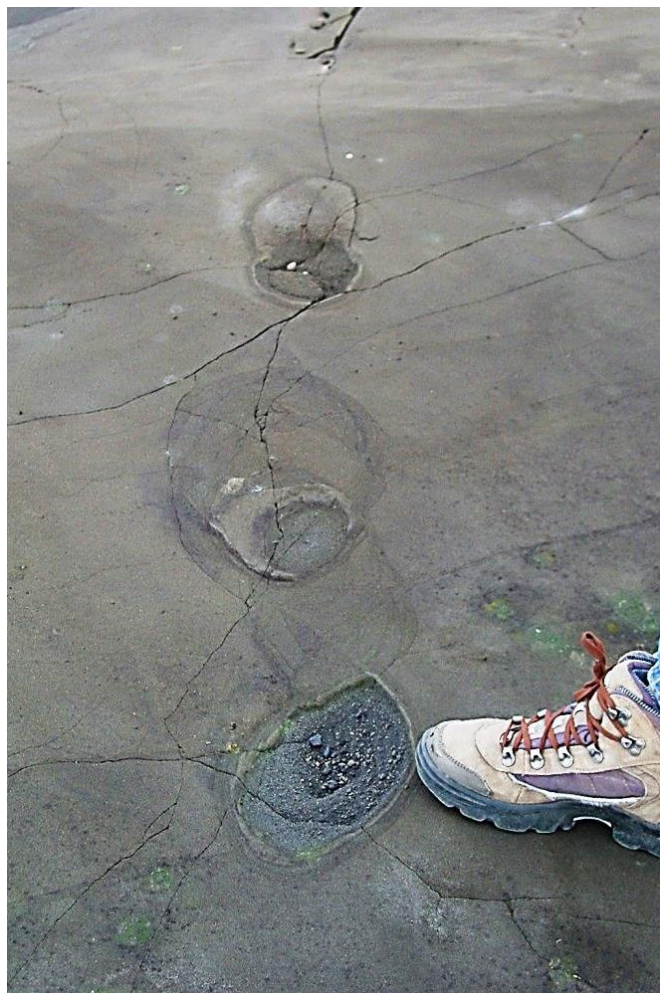
D



Ofærugil (West to the right) : **Member B.** A) mass flow from the Nordubjallar adventice cone ; B) faulting and ridge dyke injection in Unit B2

C) Thin (0,7 m) volcanic dyke of the Hekla below Unit B 2 ; D) aerial lacustrine episode (rythmites) deformed by small sized loadcasts.

A



B



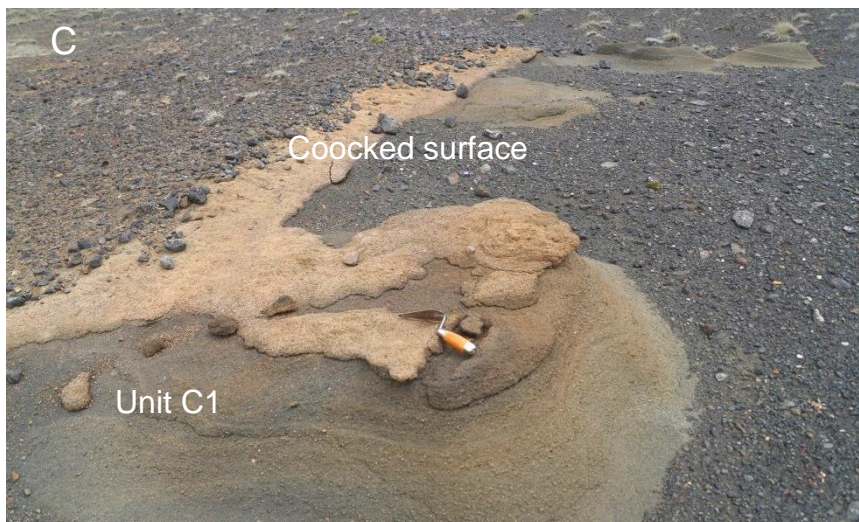
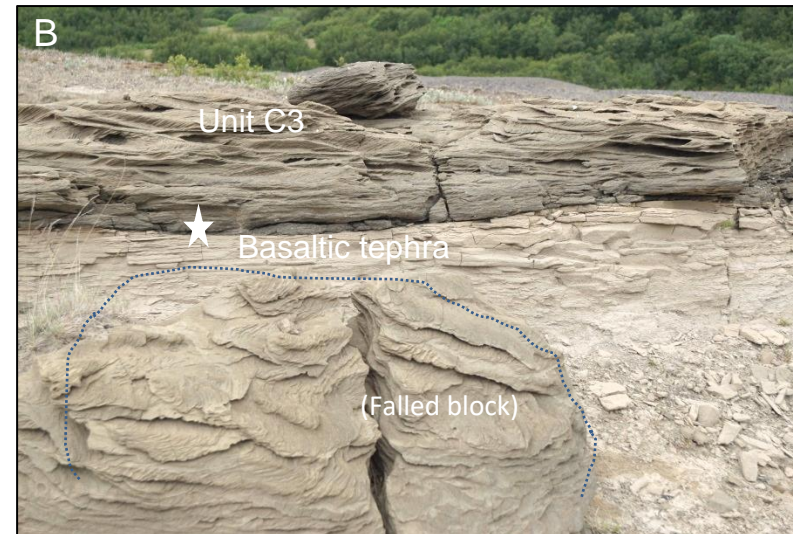
C



D



Middle Rangá valley Member C . A) small water-escape following a fracture (Hekla fault system) B) Water escape piercing unit C3b (tidal channel) C) tidalites perturbed by syndimentary clustered load cast (Unit C3a) D) Kirkubjaer : water escape lateral to the large convolute of Fig. 7B.



Hekla plinian eruption, lower Member C, to the top of C2 unit, scoured by jökulhlaup, Næfurholt. A) view of the deposit with a distal base surge (massive), reworked by flood (B) on a heated (reddened) surface (C) in association with low magnitude oriented convolute (// to the Hekla fault system). C3 unit includes rolled pumices.

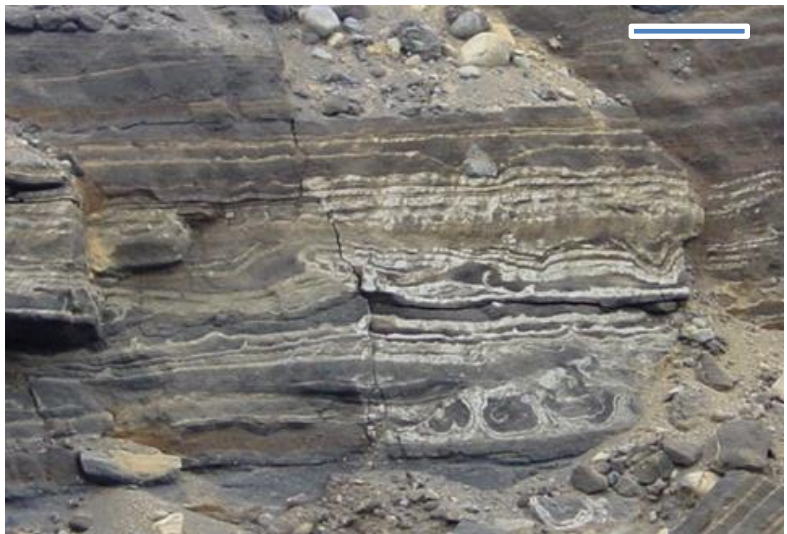
A



B



C



D



The quarry of Akbraut (Figs 1, 8) east bank of the Þjórsá River, south of the Búði moraine complex. Various Kevin-Heimholz convolutes (A-C-D) in glaciomarine silts; layer fragmentation and convolutes in lacustrine varves (B); notice fracturation (glacitectonism, 11,4 cal ka). Scale: 20 cm.



Galtalækur (Störholl): Hekla lava at the contact of C3-C4 tidal units (khaki): dated at 116 ± 10 ka by U isostopes disequilibrium . Notice the tumuli shape of the lava flow and the erosion of the sediment by the Holocene jökulhlaups (residual pillars).

A



B



C



D



Present-day earthquake and Bitra Earthquake (2000) : A) small water escape $M_w < 4$ at Snæfellsness; Bitra earthquake: B) lateral (oblique) water escape confined below a road (left to the grass); C) earthquake collapsed thufurs (empty vegetal envelope); C) large sand blow in a water-saturated depression.

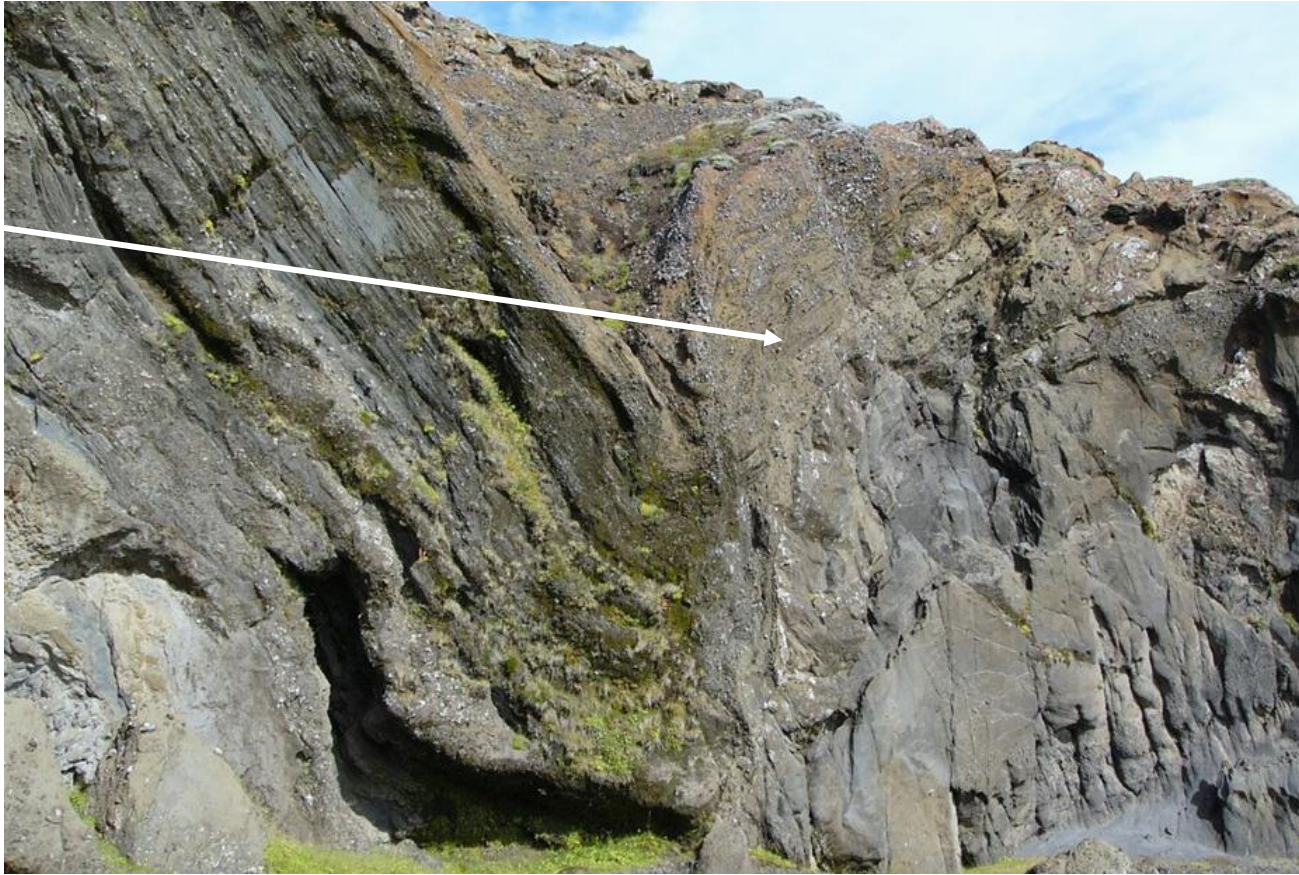


Hellutindar Ridge and Kleifarvatn

- ☆ Hellutindar and the two peninsula : Innrístapi (the smallest) and Sydrístapi, the sharpest. Notice higher and more dismantled summits to the SW, the edge of the former ice sheet



Kleifarvatn: collapsed popdown in non-oxydised hyaloclastite, East of Innristapi; along a N170° SISZ fault: syn sedimentary fault activity close to 155 ka. Notice to the right the parallel fracturation within the hyaloclastite



Háuhnúkar Tindar in the background above the quarry. Notice the graben at the northern end of the quarry (Fig.8C) and the extensive fault on the right in the pillow-lava wall (unsuccessful dating). The upper platform is mostly in pillow breccia and is lapped on by hyaloclastites.

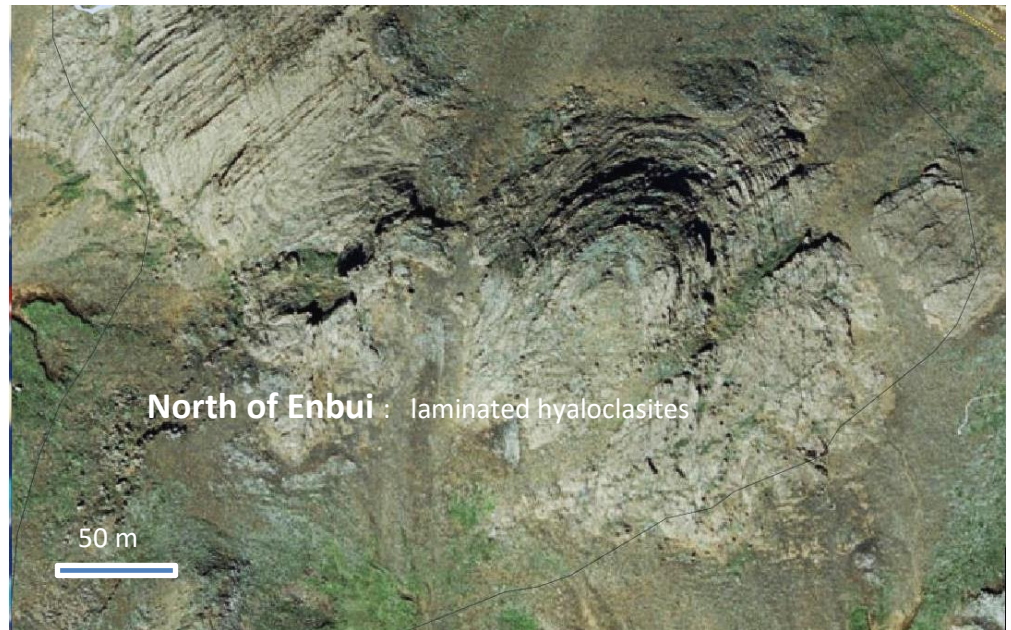


Hellutindur dating site . scoria , interstratified lava, pillow breccia
 N63°56'43.3" W63°56'43.3" , 146 masl



North of Enbui : laminated hyaloclastites

50 m



Kleifarvatn sedimentary facies:



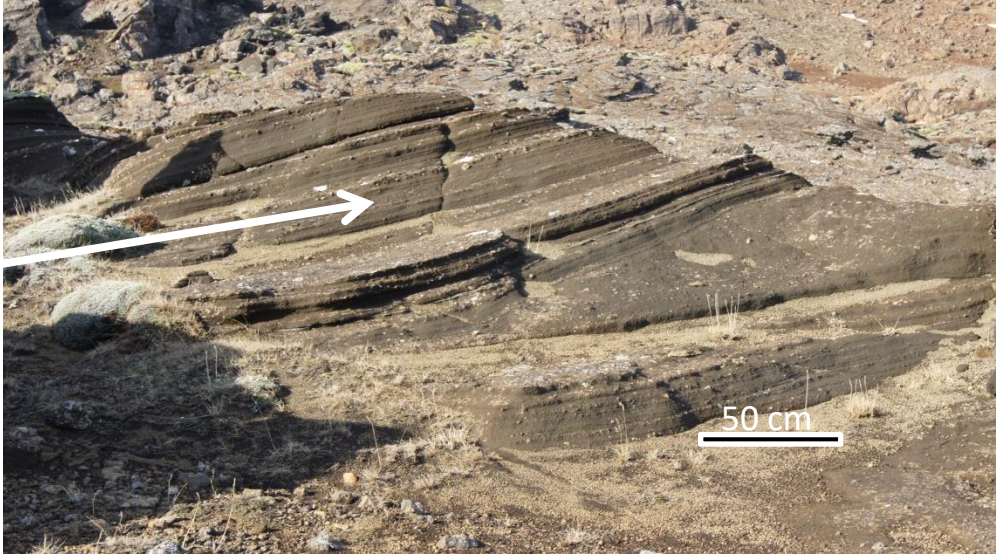
Sloped wash , above Syðristapi : equivalent of Units C1-C2



Dropstone in littoral deposits : equivalent of Unit C3a



Littoral sand bar : equivalent of Unit C3a



50 cm